



Evaluation of Antibacterial Potential of Biosynthesized Plant Leave Extract Mediated Titanium Oxide Nanoparticles using *Hypheae Thiebeace* and *Anannos Seneglensis*

¹HASSAN, H; ¹OMONIYI, KI; ¹OKIBE, FG; ¹NUHU, AA; ²ECHIOBA, EG

¹Department of Chemistry, ²Department of Veterinary Medicine, Ahmadu Bello University, Zaria-Nigeria

*Corresponding Author Email: hussainahassan92@gmail.com

ABSTRACT: The need for new antimicrobial agent has drawn attention on developing new and emerging materials based on nanoparticles with antimicrobial activity. The aim of this research was to evaluate the antibacterial activity of nanoparticles of titanium dioxide. A green synthesis of TiO₂ nanoparticles was done using a plant extract of *H. thelbiecea* and *Ananos seneglensis*. The presence of various photochemical like flavonoids, steroids, polyphenols, and terpenoids was investigated by following standard biochemical methods. The titanium oxide nanoparticles (TiO₂ NPs) synthesized was confirmed by their change of colour to brown and reddish brown due to the phenomenon of surface Plasmon resonance. The characterization studied was done by UV-vis spectroscopy, scanning electron microscopy (SEM), X-Ray diffraction (XRD) and Fourier Transmission infrared spectroscopy (FTIR). The green synthesized TiO₂ NPs excitation was confirmed using UV-Vis spectrophotometer at 270 and 290 nm. SEM revealed that the synthesized TiO₂ NPs are spherical and crystalline in nature. The overall sizes are 40 and 50 nm for *H. thelbiecea* and *Ananos* respectively. FTIR spectroscopy analysis showed the presence of flavonoid, polyphenols and amide groups likely to be responsible for the green synthesis of titanium oxide nanoparticles using *H. thelbiecea* and *Ananos seneglensis* aqueous leaf extracts. The XRD pattern showed the characteristic Bragg peaks of (111), (200), (220) and (311) facets of the anatase titanium oxide nanoparticles and confirmed that these nanoparticles are crystalline and spherical in nature. The two plants used to synthesized titanium oxide nanoparticle (*H. thelbiecea* and *ananos seneglensis*) showed good antimicrobial activity against clinically important pathogens. The antimicrobial study of TiO₂ NPs shows that 20 µg/ml TiO₂ NPs is effective for complete inactivation of Gram positive, Gram negative as well as fungal cultures. This effective microbial inactivation is mainly attributed to its ability to cause damage to the cell membrane.

DOI: <https://dx.doi.org/10.4314/jasem.v23i10.5>

Copyright: Copyright © 2019 Hassan *et al.* This is an open access article distributed under the Creative Commons Attribution License (CCL), which permits unrestricted use, distribution, and reproduction in any medium, provided the original work is properly cited.

Dates: Received: 25 September 2019; Revised: 23 September 2019; 31 October 2019

Keywords: Titanium oxide, phytochemicals, antimicrobial activity, *H. thelbiecea*, *Ananos seneglensis*

Antibiotics provide the main basis for the therapy of microbial (bacterial and fungal) infections. Since the discovery of these antibiotics and their uses as chemotherapeutic agents there was a belief in the medical fraternity that this would lead to the eventual eradication of infectious diseases. However, overuse of antibiotics has become the major factor for the emergence and dissemination of multi-drug resistant strains of several groups of microorganisms (Chandra *et al.*, 2016). The worldwide emergence of microbial infections has become a major therapeutic problem. Multi-drug resistant strains of microbial infections are widely distributed in hospitals and are increasingly being isolated from community acquired infections (Weir *et al.*, 2012, Chang *et al.*, 2002). The field of nanotechnology is one of the most active areas of research in modern material sciences. Recent nanotechnology holds a promise and a broad aspect towards wide applications of nanoparticles in a multiple way of emerging fields of science and technology. Nanoparticles usually referred to as particles with a size approximately smaller than 1 µm, normally 1-100nm, (Christensen *et al.*, 2011). It exhibit completely new or improved properties based

on specific characteristics such as size, distribution and morphology. The nanoparticles possess unique physicochemical, optical, mechanical, diagnostic and biological properties which can be manipulated for desired applications (Christopher *et al.*, 2015). Nanoparticles are finding important applications in the field of medicine, (Dahl *et al.*, 2007). They provide solutions to technological and environmental challenges in the areas of solar energy conversion, catalyses, and water treatment (Damle *et al.*, 2016, Chung *et al.*, 2005). Nanomaterials particularly metallic nanoparticles have assumed a great deal of importance as they often display unique and considerably modified physical, chemical and biological properties as compared to their counterparts of a macro scale (Edison *et al.*, 2013). Recently, titanium dioxide nanopowder has received much interest. This is due to its use in various applications such as cosmetics, paper and medical devices coating and gas sensors (Deorsola *et al.* 2008; Kobayashi *et al.* 2008; Wang *et al.* 2008). As far as the treatment of infectious diseases is concerned, resistance has developed due to injudicious and insensible use of antimicrobial agents (Das *et al.*, 2013). From the time

of immemorial, for the cure of infections, the inorganic antimicrobials such as silver and copper have been in practice (Dehpour, 2009). Some of the new potential of nanoparticles are in the area of diagnostics and biomolecular detection of diseases as well as antimicrobials in therapeutics of infectious diseases (Jain *et al.*, 2009). Various chemical and physical methods are involving for the synthesis of nanoparticles (Deshpande *et al.*, 2011, Din *et al.*, 2015). The chemical and physical synthesis of nanoparticles is expensive and often involves the use of toxic, hazardous chemicals which may pose environmental risks (Divya *et al.*, 2015). Biological methods have been put ahead to be advantageous over other synthetic methods as they are cost effective and do not involve the use of toxic chemicals, high pressure, energy and temperatures (Djanaguiraman *et al.*, 2006, Brage *et al.*, 2005). The Nanoparticle are biosynthesized using various biosources such as bacteria, fungi, yeast, plant extract. Synthesis using bio-organisms is compatible with the green chemistry principles. The biosynthesis is eco-friendly as are the reducing agent employed and the capping agent of the reaction (Dubey *et al.*, 2009). Hence developing of reliable biosynthetic and environment friendly approach has added much importance because of its eco-friendly products, biocompatibility and economic viability in the long run and also to avoid adverse effects during their application especially in medical field. Among the biological alternatives, plants and plant extracts seem to be the best option. Plants are nature's "chemical factories". They are cost efficient and require little or no maintenance. A vast repertoire of secondary metabolites is found in all plants which possess redox capacity and can be exploited for biosynthesis of nanoparticles. As a wide range of metabolites are presented in the plant products/extracts, nanoparticles produced by plants are more stable and the rate of synthesis is faster in comparison to microorganisms. Thus, the advantages of using plant and plant-derived materials for biosynthesis of metal nanoparticles have instigated researchers to investigate mechanisms of metal ions uptake and bio reduction by plants, and to understand the possible mechanism of metal nanoparticle formation in and by the plants. Biosynthesis of nanoparticles is a bottom up approach where the main reaction occurring is reduction/oxidation. The plant phytochemicals reducing properties are usually responsible for the preparation of metal and metal oxide nanoparticles. Recently nanoparticle synthesis were achieved using plant extract such as *azadirachta indica*, *camellia sinensis*, *Nyctanthes arbor-tristis*, *coriandrum*, *nelumbo nucifera*, *ocimum sanctum* and several others which is compatible with the green chemistry principles.. The main phytochemicals

responsible for the synthesis of nanoparticles are terpenoids, flavones, ketones, aldehydes, amides (Dwivedi *et al.*, 2010). The present work is based on the plant extracts of *H. thiebicea* and *A. seneglensis* plant extract. They are medicinal plant ever known. These species are frequently cited as being used in herbal medicines since the beginning of the first century AD (Brage *et al.*, 2005).

MATERIALS AND METHODS

Sample Collection: Fresh leaves of *H. thiebicea* and *Ananos seneglensis* plants were collected from the biological garden of Federal Polytechnic, Bida, Niger State, Nigeria (Longitude 6° 00' 35.64°E, Latitude 9° 04' 49.58'N) in May 2017.

Preparation of the plant extract: The leaves of *H. thiebicea* and *Ananos seneglensis* collected were thoroughly rinsed in distilled water, and then room dried for two weeks. After which hands were used to break them into fine pieces. Then 500g of each plant was smashed into 1000 ml of sterile distilled water in a gas jar and boiled at 60°C for 15 mins and then filtered through a Whatman No.1 filter paper. The aqueous extracts were stored at 40°C in an incubator for further experiments.

Synthesis of TiO₂ nanoparticles from the extracts: From a 1.0M solution of TiCl₄ prepared, 5.0ml solution was measured using a suction pipette, and was then mixed with 100 ml of distilled water in a 250 ml Erlenmeyer flask. The preparation was swirled properly. The mixture was then stored at 40°C before use. To a 100 ml portion of each of the leaf extract of *H. thiebicea* and *Ananos seneglensis* 10 ml of 1.0M TiCl₄ solution was added drop wisely in a water bath at 70°C for a period of 4 hours with continuous stirring at 1000 rpm. The suspension produced was centrifuged at 200 rpm for 20 min and the supernatant liquid decanted off; the residue was repeatedly washed with de-ionized water. Centrifugation, decantation and washing processes were repeatedly done thrice to remove any impurity on the surface of the titanium oxide nanoparticles (Sangeetha *et al.*, 2016). The precipitate obtained was dried in an oven at a temperature of 40°C for 2 hours. The synthesized titanium dioxide nanoparticle samples were then subjected to characterization by UV- Vis, FTIR, XRD and SEM.

Uv-vis spectrophotometry determination: About 10 mg each of plant extracts only, extracts mediated titanium oxide nanoparticles and commercial TiO₂ nanoparticles samples in colloidal solutions were separately placed in the cell holder of a UV- Vis spectrophotometer (model UV 1800 Shimadzu, Japan),

in order to determine the absorption spectrum of the sample using the range between 200 to 800 nm. Colloidal solution was obtained by mixing warm distilled water with synthesized TiO₂.

Fourier transforms infrared spectroscopy (FTIR) analysis: The determination of the functional groups in the plant extract, and synthesized plant extract mediated titanium oxide nanoparticles was carried out using FTIR spectrophotometer ((Perkin Elmer Spectrum 2, Germany) in the range of 4000–400 cm⁻¹ at a resolution of 4 cm⁻¹. The samples were prepared by dispersing each of the biosynthesized titanium oxide NPs or commercial TiO₂ nanoparticles uniformly in a matrix of dry KBr, and then compressed to form an almost transparent disc. KBr was used as a standard analyte for the samples according to the method of Dhadapani *et al.* (2012).

Scanning electron microscopy (SEM) of the nanoparticle: SEM machine (HITACHI Model S-3000H Japan) was used at South Africa in August 2018 to determine the surface morphology of the synthesized nanoparticles. Thin films of the samples (biosynthesized titanium oxide NPs and commercial TiO₂ nanoparticles) were prepared on a carbon coated copper grid by dropping a very small amount of each sample on the grid, the film on the SEM grid was allowed to dry and the images of the nanoparticles taken.

X-ray diffraction (XRD) analysis of the nanoparticles: X-ray diffraction measurements of the biosynthesized titanium oxide NPs and commercial TiO₂ nanoparticles were recorded on X-ray diffractometer (Philips PAN analytical machine, South Africa). The phase variety, particle size and material identification of the NPs were identified.

Evaluation of Antibacterial Activities

Antibacterial activity: The anti-bacterial action of the synthesized plant extract mediated titanium dioxide nanoparticle, plant extracts and commercial TiO₂ nanoparticles were determined by the well-diffusion technique. The action against four clinical pathogens (*Bacillus subtilis*, *Staphylococcus aureus*, *Escherichia coli*, *Salmonella typhi*) was carried out using 6 mm wells being cut on Mueller-Hinton agar swabbed with individual pathogenic bacteria according to the method of Choi *et al.* (2010). Four wells were cut in each plate where 50 ml/mg, 75 ml/mg, and 100 ml/mg of colloidal solution of as-synthesized nanoparticles, plant extracts and commercial TiO₂ nanoparticle were added separately.

Each of the biosynthesized TiO₂ nanoparticle was dissolved in warm distilled water and allowed to form colloidal solution. One well was maintained as control by adding sterilized distilled water, while to another group, Ampicillin manufactured by Alcimpil FN. (Farcoral, Mexico) was added to serve as standard drug. The plates were incubated for 24–48 hr and checked for the zone of inhibition using the method of Anusha *et al.* (2011).

The experiments were carried out in triplicate. The results (mean value, n=3) were recorded by measuring the zones of growth inhibition surrounding the disc.

Determination of Minimum Inhibitory Concentration (MIC): The minimum inhibitory concentration of the extracts of *H. thelwiecea* and *Ananos senegalsisa* mediated TiO₂ nanoparticle, commercial TiO₂ nanoparticle and plant extract were determined using tube dilution method with Mueller Hinton broth used as diluents. The lowest concentration of the sample showing inhibition for each organism when the samples were tested for sensitivity was serially diluted in the test tubes containing Mueller Hinton broth. The organisms were inoculated into each tube containing the broth and the extracts. The inoculated tubes were then incubated at 37°C for 24 hours. At the end of which the tubes were examined for the presence or absence of growth using turbidity as a criterion, the lowest concentration on the series without visible sign of growth (turbidity) was considered to be the minimum inhibitory concentration (MIC).

Determination of Minimum Bacteriocidal Concentration (MBC): The result from the minimum inhibitory concentration (MIC) was used to determine the minimum bacteriocidal concentration (MBC) for the samples. A sterilized wire loop was dropped into the test tube (s) that did not show turbidity (clear) in the MIC test and a loopful was taken and streaked on a sterile nutrient agar plates. The plates were incubated at 37°C for 18–24 hours. At the end of incubation period, the plates were examined/observed for the presence or absence of growth. This is to determine whether the antimicrobial effect of the samples are bacteriostatic or bacteriocidal (Feizi *et al.*, 2013).

Determination of minimum fungicidal concentration (MFC): The MFC of The biosynthesized TiO₂ NPs using the plant extract, commercial TiO₂ nanoparticle and plant extracts were determined using the method of Raymond *et al.* (2009). The MIC test tube was sub-cultured on fresh sterile Sabouraud dextrose agar plate and incubated at 28°C for 24–72 hour. Presence of growth after the period of incubation was interpreted

as bacteriostatic while the absence of growth was considered fungicidal.

Statistical analysis: The experimental results were expressed as mean + standard deviation (SD) of three replicates. The data were subjected to one-way analysis of variance ANOVA and differences between sample were determined by two tailed t-test after Bonferroni error correction of the predictive values. P value less than 0.005 were considered statistically significant. Microsoft Excel 2010 statistical package was used for all analysis.

RESULTS AND DISCUSSION

UV visible analysis: The UV-Vis spectroscopy was used to determine the formation and the stability of the synthesized titanium oxide nanoparticles in aqueous colloidal solution. It is also used to predict the initial phyto-constituents in plant material. The UV spectrum of the prepared biosynthesized TiO₂ nanoparticles, commercial titanium oxide Nps and plant extracts presented in Figure 1, 2 and 3 indicated that they all display maximum absorption in the vicinities of 400 - 800 nm. The spectrum showed the formation of peak in the wavelength of 229 nm for the *A. senegalesis* mediated NPs, a peak in the wavelength of 231 nm for the *H. theibeacea* mediated counterpart, a peak of 430 nm for commercial titanium oxide nanoparticles respectively. The absorptions are as follows: 3.475, 3.678 and 1.27 nm for *A senegalesis* mediated NPs, *H. theibeacea* mediated NPs and commercial titanium oxide nanoparticles respectively (Kim *et al.*, 2013). The UV-Vis spectra of plant extracts of *A. senegalesis* mediated TiO₂ Nps and plant extracts of *H. theibeacea* mediated TiO₂ Nps have high absorbance intensity compared to commercial titanium oxide nanoparticles. This is because, various metabolites from plant extract introduced to solution make the plasmon band broad and they may be read in the spectrophotometric with surface plasmon resonance (SPR) was responsible for exhibiting the absorption of UV-Vis radiation (Kim *et al.*, 2013). These wave lengths arise due to the surface Plasmon resonance of the particle (Joshin *et al.*, 2008). The magnitude of peak, wavelength and spectral bandwidth associated with nanoparticles are dependent on size, shape and material composition (Prakash *et al.*, 2013, Kim *et al.*, 2013). These changes in their properties increases their interacting faces thereby considered as enhancement in terms of absorption of wave length spectrum in the UV-Vis region.. Commercial TiO₂ Nps had the least absorption. As indicated in Figure 4 and 5 .This was similar to the trend obtained by Salam *et al.*, (2016) in the work done on synthesised Citrus paradi peel extract mediated titanium dioxide nanoparticles. and

biological synthesis of TiO₂ nanoparticles using extracts of *Ananas comosus* (Anwar *et al.*, 2010, Wilkinson *et al.*, 2011).

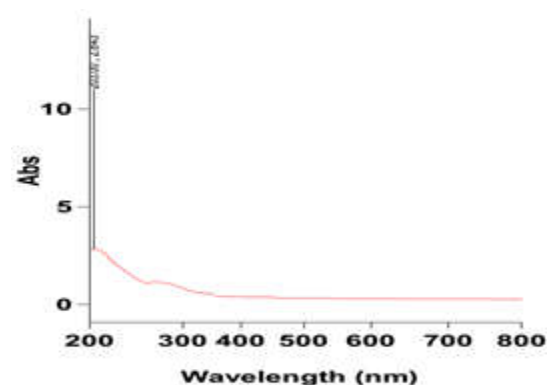


Fig 1: UV-Vis spectra of titanium oxide nanoparticles synthesized by *H. theibeacea*

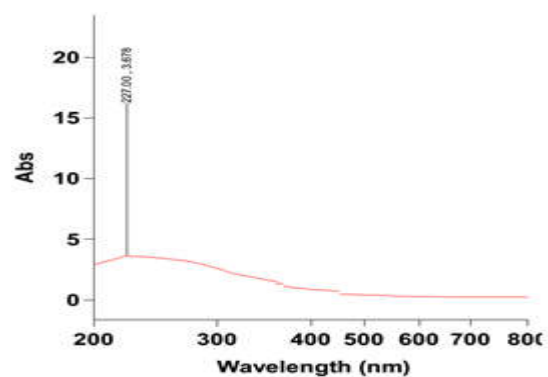


Fig 2: UV-Vis spectra of titanium oxide nanoparticles synthesized by *A. senegalesis*.

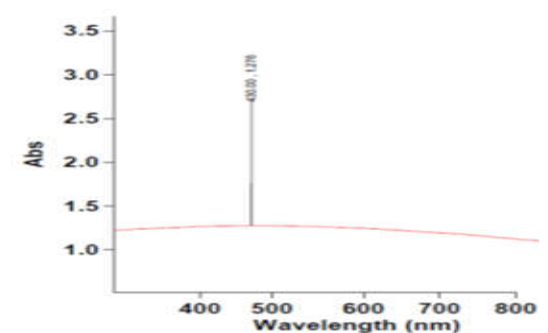


Fig 3: U-visible spectrum of commercial titanium oxide of nano particle

Fourier Transform Infrared Spectroscopic Study: FTIR analysis was used to find out the reduction of TiO₂ nanoparticles by biomacro molecules present in the plant extract. These biomacro molecules are responsible for the reduction and stabilization of TiO₂ nanoparticles. Figure 4, 5 and 6 shows the FT-IR spectrum of *H. theibeacea* mediated TiO₂ NPs, *A.*

senegalensis mediated TiO₂ NPs and that for commercial TiO₂ NPs, respectively.

H. theibiecea mediated TiO₂ NPs: The characteristic absorption bands were exhibited at 2920cm⁻¹ (for C-H stretching) and at 1602.8 cm⁻¹ for carbonyl group (C=O), and at 3678.9 cm⁻¹ for Hydroxyl (-OH) group; Amine at 2920 cm⁻¹ and 1513 cm⁻¹ for (C=C) stretching vibration.

A. senegalensis mediated TiO₂ NPs: *A. senegalensis* mediated TiO₂ NPs showed characteristic absorption bands at 3220cm⁻¹ for hydroxyl (-OH) group, 1617cm⁻¹ (for C=O) stretching), absorption at 1282 cm⁻¹ (for C-N stretching) and at 1438 cm⁻¹ for alkyl group.

Commercial TiO₂ NPs: Figure 6 indicated commercial TiO₂ Nps characteristic absorption bands were exhibited at 3712 - 3768cm⁻¹ for hydroxyl (-OH) group and at 1654 cm⁻¹ for carbonyl group (C=O). From the FTIR results (Figure 10) there is presence of hydroxyl groups of phenols, carbonyl group (C=O), alkyl group. Bali *et al.* (2006) reported same with also amide group, these form layers on the nanoparticles and acting as a capping agent to prevent agglomeration and providing stability in the medium in the work on extract of *N. tabacuum* Leaves mediated silver Nps. The functional groups in the FTIR results support the presence of phenolic compounds (flavonoids) in the extracts as evidenced by phytochemical analysis. Raymond *et al.* (2009) reported that the band at 1742 cm⁻¹ is characteristic of stretching vibrations of the carbonyl functional group in ketones, aldehydes and carboxylic acids in the study on *Micrococca mercurialis*

Table 1. FTIR absorption frequencies of plant leaf extract mediated TiO₂ nanoparticles. Assignments of FTIR peaks of HT and AS
Note: ,HT = *H. theibiecea* and AS = *Annonas senegalensis*

Wavenumber (cm ⁻¹)	Assignments
AS	
3257.7	O-H stretching vibration
2926.0	Asymmetric C-H stretching
2113.4	overtone and/or combinational bands
1606.5	C=C aromatic
1438.8	C-H in-plane deformation
1375.4	C-H symmetric deformation
1282.2	C-O stretch
1073.5	C-O asymmetric stretch
HT	
3220.4	O-H stretching mode
2113.4	overtone and/or combinational bands
1617.7	C=C aromatic
1524.5	C=C aromatic
1438.8	C-H in-plane deformation
1282.2	C-O asymmetric stretch
1110.7	C-O stretch

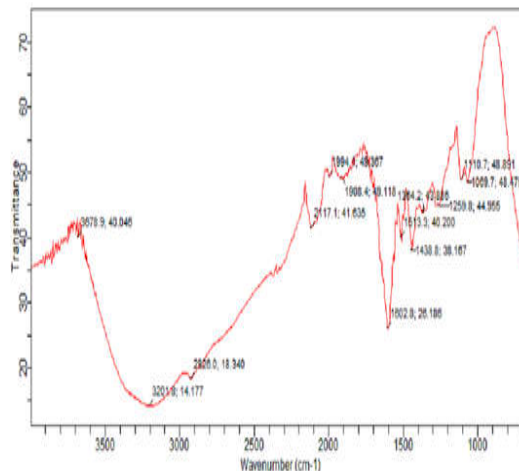


Fig 4: FTIR spectra from solid powder titanium oxide nanoparticles by *H. theibiecea* extract

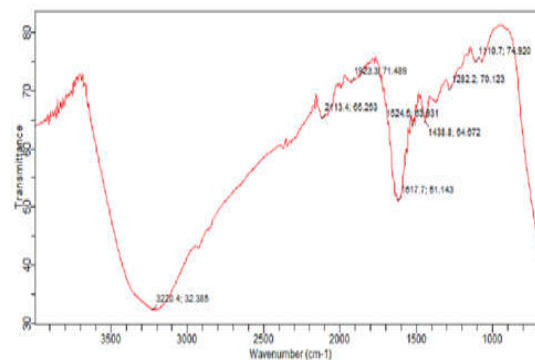


Fig 5: FTIR spectra from titanium oxide nanoparticles by *A. senegalensis*.

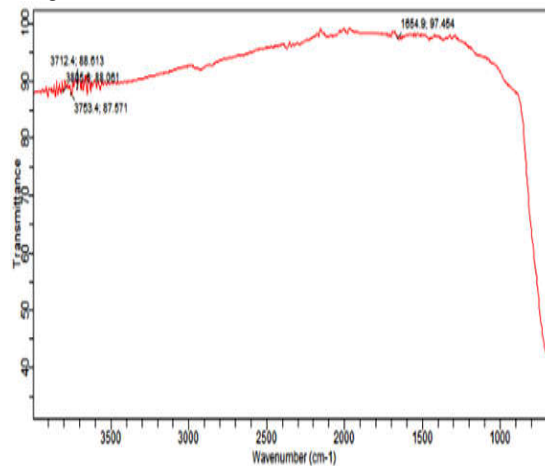


Fig 6: FTIR spectra from by Fine commercial powdered titanium oxide nanoparticles

Based on these FTIR studies, it can be suggested that the bio-molecules present in the plant extracts of *H. theibiecea*, *A. senegalensis* plant extracts. Then plant extract mediated TiO₂ Nps of *H. theibiecea* and *A. senegalensis* play dual role in formation and stabilization to TiO₂ nanoparticles

Scanning Electron Microscopic analysis: Fig. 7, 8 and 8 shows the SEM images of biosynthesized TiO₂ nanoparticles obtained using leaf extracts of *H. thelbigcea*, *A. senegalensis* and commercial TiO₂ nanoparticles respectively. The image describes the surface morphology of the TiO₂ nanoparticles. The green synthesized TiO₂ nanoparticles showed monodispersity without aggregation when compared to that of the commercial TiO₂ nanoparticles. This is due to the capping of TiO₂ nanoparticles with the compounds present in the leaf extract. The particles were found to be spherical with distinct edges and without aggregation. Previous reports showed that phytochemical compound in nanoparticles are disaggregated and are stable with good dispersibility. Prathna *et al.* (2010) supports the present findings in the work on *The Origanum vulgare* aqueous leaf extract. It could therefore be speculated that the phytochemicals in these leaf extracts coats the surface of the TiO₂ nanoparticles thus preventing their aggregation. The SEM images showed average sizes of 50 nm, 40 nm and 72nm for biosynthesized TiO₂ nanoparticles obtained using leaf extracts of *H. thelbigcea*, *A. senegalensis* and commercial TiO₂ nanoparticles respectively. The images showed that the samples are spherical in shape. Titanium dioxide nanoparticle of approximate diameter 50-60 nm have been previously reported (Raymond *et al.*, 2009). The TiO₂-NPs, of these sizes showed that nanoparticles produced by this method were primarily crystalline (Wang *et al.*, 2005; Ismajijov *et al.*, 2009).

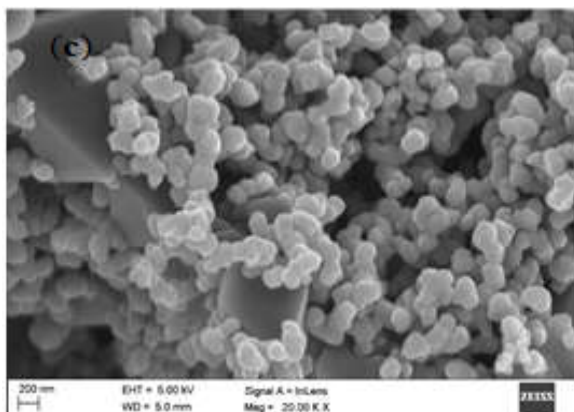


Fig 7: Scanning electron microscopy image of the biosynthesis of TiO₂ nanoparticle by *H. thelbigcea*.

The XRD pattern of TiO₂ nanoparticles obtained using flower extract of *H. thelbigcea* and *A. senegalensis* are shown in Fig. (10, 11 and 12) A sharp diffraction peak was observed with slight broadening peak for green synthesized TiO₂ nanoparticles. The lattice parameters obtained were close and consistent with standard data for TiO₂ (JCPDS 21-1272) (Vijayalakshmi *et al.* 2012). We have calculated the average crystallite size

of TiO₂ nanoparticles synthesized by green route using the Scherrer's formula ($d = 0.89 \lambda / \beta \cos\theta$).

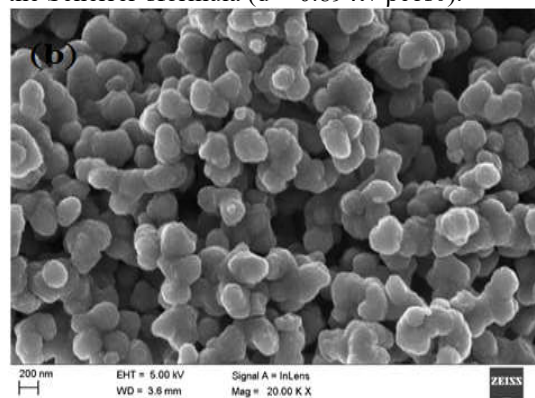


Fig 8 Scanning electron microscopy image of the biosynthesis of TiO₂ nanoparticle by *A. senegalensis*.

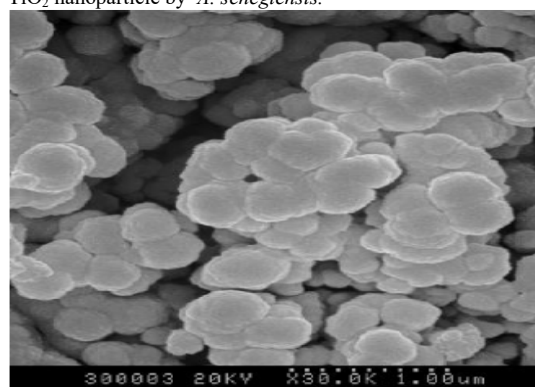


Fig 9; Scanning electron microscopy image of the Commercial TiO₂ nanoparticle by *A. senegalensis*

The calculated crystallite was found to be 58nm,43nm,45nm and 42 nm respectively. nm for green synthesized TiO₂ nanoparticles. The results of XRD analysis confirm the presence of TiO₂ nanoparticles in the green synthesised sample. Previous reports have also used XRD as an evidence for the confirmation of TiO₂ nanoparticles (Li *et al.* 2006). The XRD peaks of green synthesised TiO₂ nanoparticles obtained using the above extract. Naheed Ahmad *et al.* (2012) have reported the correlation between XRD peak broadening and the size reduction during green synthesis protocol. Thus, the broadening of XRD peak of green synthesised TiO₂ nanoparticles observed in our study confirms the size reduction. Earlier reports on XRD data of nanoparticles have documented an inverse relation between peak intensity and surface functionalization of nanoparticles (Daizy Philip, 2009). Surface coating of the nanoparticles with functional groups (i.e, surface functionalization) results in an internal strain in the particles consequently decreasing the signal: noise ratio. As a result, the intensity of the XRD peak decreases (Kannan *et al.* 2008). Therefore, we suggest that the phytochemicals present in the extracts would

have coated the surface of the TiO₂ nanoparticles, resulting in decreased intensity in XRD peak. This phytochemical coating may enhance the stability and the dispersibility of the nanoparticles, which in turn may enhance their bioavailability, making them suitable for biological applications. The XRD profile reveals that the green synthesis protocol that we developed using *H. thelbiecea* and *A. seneglanesises* is valid for the production of biofunctionalized and bio-stabilized titania nanoparticles with potential biomedical activities.

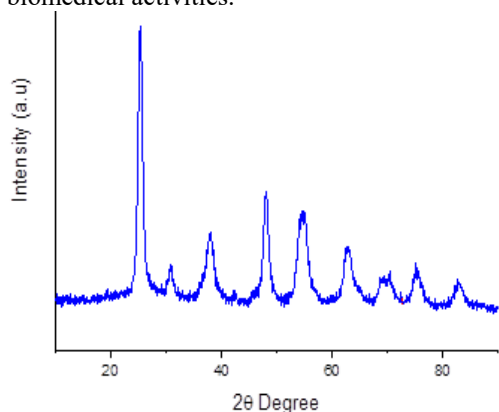


Fig 10. XRD images of biosynthesized TiO₂ NPS by *H. thelbiecea* extract.

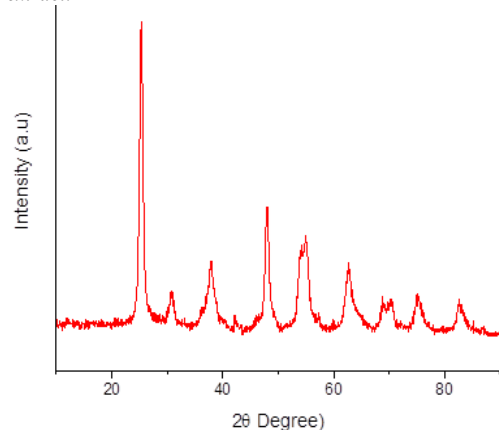


Fig 11. XRD images of biosynthesized TiO₂ NPS by *A. seneglanesises* extract.

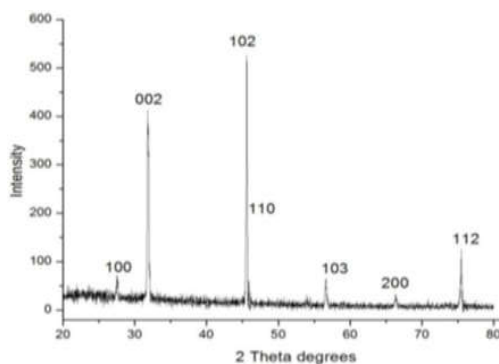


Fig 12: XRD of commercial TiO₂ nano particles

Antimicrobial activities of Nanoformulated TiO₂ NPs:

The antimicrobial activity of the extracts of *H. thelbiecea* and *A. seneglanesises* mediated TiO₂ nanoparticle was compared with that of commercial TiO₂ nanoparticle and the extracts of *H. thelbiecea* and *A. seneglanesises*, against four microbial pathogens by agar well diffusion method successfully. The antibacterial activity results revealed that the biosynthesized TiO₂ nanoparticles acted as excellent antibacterial agents against both Gram-positive and Gram-negative bacteria when compared with commercial TiO₂ nanoparticles and plant extracts of *H. thelbiecea* and *A. seneglanesises*. Tables 2, 3 and 4, and Figures 17, 18 and 19 show the values and zones of inhibitions produced by the green synthesized TiO₂ nanoparticles, commercial TiO₂ nanoparticles and the plant extracts of *H. thelbiecea* and *A. seneglanesises* against both Gram-positive and Gram-negative bacterial strains. *H. thelbiecea* mediated TiO₂ nanoparticles exhibited maximum (15 mm) bacterial growth inhibition against *B. subtilis* while *A. seneglanesises* mediated TiO₂ nanoparticles exhibited maximum (14 mm) bacterial growth inhibition against *B. subtilis*, in the form of zone-of-inhibition studies, where diffusion of nanoparticles on nutrient agar plates inhibits growth. In contrast, the commercial TiO₂ nanoparticles showed zones of inhibition of 11 mm against *B. subtilis* and plant extracts showed 10.5 mm. In the case of *E. coli* maximum growth inhibition zones were found to be as follows: 17, 12, 8 and 7 mm for *H. thelbiecea* and *A. seneglanesises* leaf extract mediated TiO₂ nanoparticles, commercial nanoparticles TiO₂ and plant extracts respectively. Similar patterns were observed in the case of *S. aureus*, where the maximum zone of inhibition was exhibited by *H. thelbiecea* a TiO₂ nanoparticles followed by *A. seneglanesises* TiO₂ nanoparticles and commercial nanoparticles TiO₂. Plant extracts of *H. thelbiecea* and *A. seneglanesises* showed zones of inhibition of 10.5 mm against *B. subtilis*.

Nanoparticles tend to adsorb on the bacterial cell and undergo dehydrogenation due to respiration process which occurs at the cell membrane of bacteria. Biosynthesized Titanium oxide nanoparticles and commercial nanoparticles TiO₂ have shown antibacterial activities more than the extract of *H. thelbiecea* and *A. seneglanesises* alone, because they have very large surface area to volume ratio, having high surface area to volume ratio in nanocrystals can lead to unexpected properties, increasing their reactivity tremendously as they have a greater number of reaction sites and can provide better contact with microorganisms.

Table 2: Antibacterial activity of nanoformulated Titanium Oxide NPs. Data are express as Mean \pm SEM of triplicate determination. Values followed by different superscript alphabet were significantly different ($p < 0.05$)

Plant extract/ concentration (mg/mL)	Test organisms/zone of inhibition (mm)			
	<i>Staphylococcus aureus</i>	<i>Bacillus subtilis</i>	<i>Escherichia coli</i>	<i>Salmonella typhi</i>
<i>H. theibiecea</i>				
100	0	0	18.65 \pm 0.32 ^c	16.45 \pm 0.33 ^b
50	0	0	16.05 \pm 0.94 ^b	14.65 \pm 0.92 ^{ab}
25	0	0	14.67 \pm 0.93 ^{ab}	12.06 \pm 0.14 ^a
12.5	0	0	12.56 \pm 0.23 ^a	11.54 \pm 0.52 ^a
<i>A. senegleensis</i>				
100	18.05 \pm 0.26 ^c	0	0	16.54 \pm 0.55 ^b
50	16.67 \pm 0.26 ^b	0	0	14.67 \pm 0.17 ^{ab}
25	14.76 \pm 0.50 ^{ab}	0	0	13.83 \pm 0.43 ^{ab}
12.5	12.04 \pm 0.27 ^a	0	0	11.43 \pm 0.55 ^a

Data are express as Mean \pm SEM of triplicate determination. Values followed by different superscript alphabet were significantly different ($p < 0.05$)

Table 5: MIC of nanoformulated Titanium Oxide NPs against bacteria isolates

Plant extract/ concentration (mg/ml)	<i>Staphylococcus aureus</i>	<i>Bacillus subtilis</i>	<i>Escherichia coli</i>	<i>Salmonella typhi</i>
	<i>H. theibiecea</i>			
12.5	-	-	-	-
6.25	-	+	-	-
3.125	+	+	+	+
1.5	+	+	+	+
<i>A. senegleensis</i>				
12.5	-	-	-	-
6.25	-	-	-	-
3.125	-	-	+	+
1.5	-	-	+	+

Table 3: MBC of plant extract mediated TiO₂ nanoparticle from against bacteria isolates

Plant extract/ concentration (mg/ml)	<i>Staphylococcus aureus</i>	<i>Bacillus subtilis</i>	<i>Escherichia coli</i>	<i>Salmonella typhi</i>
	<i>H. theibiecea</i>			
12.5	-	-	-	-
6.25	-	+	-	-
3.12	+	+	+	+
1.5	+	+	+	+
<i>senegleensis</i>				
12.5	-	-	-	-
6.25	-	-	-	+
3.12	-	-	+	+
1.5	-	-	+	+

Surfaces of nanoparticles affect/interact directly with the bacterial outer membrane, causing the membrane to rupture and killing bacteria due to its extremely small size. The as-synthesized TiO₂ nanoparticle had more effectiveness and efficacy against microbial activity than does the commercial TiO₂ nanoparticle, because of the capping agent (phytochemicals) from the plant extract in the as-synthesized TiO₂ nanoparticle. These are saponins, tannins, flavonion, alkaloids, phenolic compounds, terpenoids, etc. These are plant metabolites known for antimicrobial activity (Ikigai *et al.*, 1990). The antimicrobial activity in terms of inhibition zone significantly varied with test microbes and the type of the extracts. Although the as-

synthesized TiO₂ nanoparticles and commercial TiO₂ nanoparticle in the present study were observed to have strong antimicrobial potential, plant extracts of *H. theibiecea* and *A. seneglanesises* were found to be less active against the tested bacterial. Effectiveness of plant extracts depends on their active compound, for example, some of them like flavonoid, tannins and terpenoids are highly soluble in water but have low absorption capacity because they are unable to cross the lipid membrane of the cells. They have excessively high molecular size or are poorly absorbed resulting in loss of bioavailability and efficacy. Some have low solubility, poor permeability and instability in biological environment. This limitation can be

overcome by encapsulating or attaching them with material known as nanomaterials. When the result was compared with the antibiotics like Ampillicin, Tobramycin and Erythromycin, nanoparticles were found to be more potent than antibiotics.

Conclusion: The present study reports the biosynthesis of TiO₂NPs, by *H. theibiecea* and *A. seneglensis* leaf extract, confirmed by XRD, UV-vis spectroscopy and FTIR analyses. Antimicrobial activities of the biosynthesized TiO₂NPs were evaluated towards pathogenic bacteria. The Bio-synthesized TiO₂ nanoparticles exhibited higher antibacterial activity against pathogenic bacteria compared to commercial TiO₂ and the plant extracts. Based on these results, it is concluded that the leaf extracts stabilized TiO₂ nanoparticles and this made it to have higher potential biomedical applications when compared to commercial TiO₂ nanoparticles. These studies would certainly be useful for the development of TiO₂NPs as an effective antifungal and antimicrobial agent against drug resistant micro-organisms.

REFERENCES

- Campostrini, R; Ischia, M; Palmisano, L. (2003). Pyrolysis study of Sol-gel derived TiO₂ powders: Part I. TiO₂- anatase prepared by reacting titanium (IV) isopropoxide with formic acid. *J. Therm. Anal. Calorim.*, 71 (3): 997- 1010.
- Chandra, S.E; Krishna R; Rao, K; Kumar, S.P. (2016) A green approach to synthesize controllable silver nanostructures from *Limonia acidissima* for inactivation of pathogenic bacteria *Cogent Chem.*
- Chang, C; Yang, M; Wen, H; Chen, J. (2002) Estimation of total flavonoid content in *Propolis* by two complementary colorimetric methods. *J. Food Drug Anal.*, 10: 178–182.
- Christensen, L; Vivekanandhan, S; Misra, M; Mohanty, A.K. (2011) Biosynthesis of silver nanoparticles using *Murraya koenigii* (curry leaf): an investigation on the effect of broth concentration in reduction mechanism and particle size. *Adv. Mat. Lett.*, 2: 429–434.
- Christopher, J; Banerjee, S; Panneerselvam, E; (2015) Optimization of parameters for biosynthesis of silver nanoparticles using leaf extract of *Aegle marmelos*. *Braz. Arch. Biol. Technol.*, 58: 702–710
- Chung, I.M; Park, ; Seung-Hyun, K; Thiruvengadam, M; Rajakumar, G. (2016) Plant mediated synthesis of silver nanoparticles: their characteristics properties and therapeutic applications. *Nanoscale Res. Lett.*, 11: 1–14.
- Dahl, J.A; Maddux, B; Hutchison, J.E. (2007) Toward greener nanosynthesis *Chem. Rev.* 107: 2228–2269.
- Daizy Philip, Biosynthesis of Au, Ag and Au–Ag nanoparticles using edible mushroom extract, *Spectrochimica Acta Part A: Molecular and Biomolecular Spectroscopy*, 374–381(2009).
- Damle, P; Hegde, D; Nayak, S; Vaman, C.R. (2016) Green synthesis of silver nanoparticles from *Santalum album* tender leaf extract and evaluation of its antioxidant capacity. *IJACS*, S1: 253–257. 140.
- Daniel, S; Ayyappan, S; Philiphan, N; Sivakumar, M; Menaga, G; Sironmani, T (2011) Green synthesis and transfer of silver nanoparticles in a food chain through Chiranamous larva to zebra fish – a new approach for therapeutics. *Int. J. NanoSci. Nanotechnol.*, 2: 159–169.
- Das, J; Das, M.P; Velusamy, P. (2013) *Sesbania grandiflora* leaf extract mediated green synthesis of antibacterial silver nanoparticles against selected human pathogens. *Spectrochim. Acta A Mol. Biomol. Spectrosc.*, 104: 265–270.
- Dehpour, A; Ebrahimzadeh, M; Nabavi, S; Nabavi, S.M. (2009) Antioxidant activity of methanol extract of *Ferula assafoetida* and its essential oil composition. *Grasas Aceites.*, 60: 405–412.
- Din, L; Mie, R; Samsudin, M; Ahmad, A; Ibrahim, N. (2015) Biomimetic synthesis of silver nanoparticles using the lichen *Ramalina dumeticola* and the antibacterial activity. *MJAS*, 19: 369–376.
- Divya, P. and Nithya, T. (2015) Silver nanoparticles eco-friendly synthesis by ornamental flower extracts and evaluation of their antimicrobial activity. *IJRPNS*, 4: 250–259.
- Djanaguiraman, M; Sheeba, J; Shanker, A; Devi, D; Bangarusamy, U. (2006) Rice can acclimate to lethal level of salinity by pretreatment with sublethal level of salinity through osmotic adjustment. *Plant Soil*, 284: 363–373 141.
- Dubey, M; Bhadauria S; Kushwaha B. (2009) Green synthesis of nanosilver particles from extract of *Eucalyptus hybrida* (safeda) leaf. *Dig. J. Nanomater. Biostruct.*, 4: 537–543.
- Dwivedi, A; and Gopal, K. (2010) Biosynthesis of silver and gold nanoparticles using *Chenopodium album* leaf extract. *Colloids Surf. A. Physiochem. Eng. Asp.*, 369: 27–33
- Edison, T; and Sethuraman, M; (2013) Biogenic robust synthesis of silver nanoparticles using *Punica*

- granatum* peel and its application as a green catalyst for the reduction of an anthropogenic pollutant 4-nitrophenol. *Spectrochim. Acta A Mol. Biomol. Spectrosc.*, 104: 262–264.
- Ismagilov, Z; Tsykoza, L; Shikina, N; Zarytova, V; Zinoviev, V; Zagrebnyi, S; (2009). Synthesis and stabilization of nano-sized titanium dioxide. *Russ. Chemistry Research*, 78 (9) 1-13. 43.
- J. Wang, B; Mao, J; Gole,L; Burda,C; (2010). Visiblelight- driven reversible and switchable hydrophobic to hydrophilic nitrogen doped titania surfaces: correlation with photocatalysis. *Nanoscale*. 2: 2257-2261.
- Jain, D; Daima, H; Kachhwaha, S; Kothari, S; (2009). Synthesis of plant-mediated silver nanoparticles using papaya fruit extract and evaluation of their anti-microbial activities. *Digest J. Nanomat. Biostru.*, 4, 557-63
- Jain, D., Daima, H.K., Kachhwaha, S., Kothari, S.L., (2009). Synthesis of plant-mediated silver nanoparticles using papaya fruit extract and evaluation of their anti microbial activities. *Dig. J. Nanomat. Bios*. 4, 557–563.
- Kannan, P. and John, S. A., Synthesis of mercaptothiadiazole-functionalized gold nanoparticles and their self-assembly on Au substrates, *Nanotechnology*, 18, 085602(2008).
- Kim, D.H., Ryu, H.W., Moon, J.H; Kim, J. (2013). Effect of ultrasonic treatment and temperature on nanocrystalline TiO₂. *Journal of Power Sources*, 163 (1): 196-200.
- Li, L., Sun, X., Yang, Y., Guan, N. and Zhang, F.,(2006). Synthesis of anatase TiO₂ nanoparticles with beta-cyclodextrin as a supramolecular shell, *Chem Asian J.*, 1, 664-8Li, Y., White, T. J. and Lim, S. H., Low-temperature synthesis and microstructural control of titania nano-particles, *J. Solid State Chem.* 177, 1372 (2004).
- Liu, C.M., L. Guo, H.B. Xu, Z.Y. Wu, and J. Weber, (2013) Seed mediated growth and properties of copper nanoparticles, nanoparticle 1D arrays and nanorods. *Microelectronic Engineering*. 66: 107-114.
- Luo, P. G., Tzeng TR, Shah RR, Stutzenberger FJ. (2007) Nanomaterials for Antimicrobial Applications and Pathogen Detection. *Curr Trends in Microbiol.*; 3:111-128.
- Mohammad, S. H., Soheil S. & Somaye, J. (2012). “The Size Effect of TiO₂ Anatase Nanoparticles on Photon Correlation Spectroscopy” *Soft Nanoscience Letters*, (2012)
- Naheed Ahmad and Seema Sharma, Green Synthesis of Silver Nanoparticles Using Extracts of *Ananas comosus*, *Green and Sustainable Chemistry*, 2, 141-147(2012).
- Prathna.V, Chandrasekaran, N A.M. Raichurb (2010) *Colloids and Surfaces B: Biointerfaces*, , (82) 152–159.
- Raymond, F.H.J., Nianqiang, W., Dale, P., Mary, B., Michael, W. & Andrij, H. (2009). Particle length-dependent titanium dioxide nanomaterials toxicity and bioactivity. Part. *Fibre Toxicol.* 6 (12): 1-11.
- Salam, H.A.; Rajiv, P.; Kamaraj, M Kudhier, M.A. (2016). Synthesis and photocatalytic activity of TiO₂ nanoparticles prepared by sol–gel method. *J. Solution Gel Sci. Technol.* 78:299-306.
- Sivaranjani, P. Philominathan “Synthesize of Titanium dioxide nanoparticles using *Moringa oleifera* Leaves and evaluation of wound healing activity” *Wound Medicine*, (2015).
- Vijayalakshmi, R. and Rajendran, V., Synthesis and characterization of nano-TiO₂ via different methods, *Arch of App Sci Res.*, 4, 1183- 1190 (2012).
- Wang, W., Lenggoro, I.L., Terashi, Y., Kim, T.O. & Okuyama, K. (2010). One-step synthesis of titanium oxide nanoparticles by spray pyrolysis of organic precursors. *Material Science Engineering*, 123 (3): 194-202.
- Weir A, Westerhoff P, Fabricius L, Hristovski K, von Goetz N. Titanium dioxide nanoparticles in food and personal care products. *Environ. Sci. Technol.* 2012 Feb 8; 46(4):2242-50.